Preprints (www.preprints.org) | NOT PEER-REVIEWED | Posted: 21 June 2020 doi:10.20944/preprints202006.0249.v1

TMPRSS2 Protease Inhibitors May Prolong But Heparins Accelerate SARS-CoV-2 Clearance

Shu Yuan,[1,5,*] Si-Cong Jiang,[2,5] Zhong-Wei Zhang,[1,5] Zi-Lin Li,[3,5] Chang-Quan Wang,[1] Ming Yuan,[4] Yang-Er Chen,[4] Qi Tao,[1] Ting Lan,[1] Xiao-Yan Tang,[1] Guang-Deng Chen,[1] and Jian Zeng[1]

[1]College of Resources, Sichuan Agricultural University, Chengdu 611130, China
[2]Chengdu KangHong Pharmaceutical Group Comp. Ltd., Chengdu 610036, China
[3]Department of Cardiovascular Surgery, Xijing Hospital, Medical University of the Air Force, Xi'an 710032, China
[4]College of Life Science, Sichuan Agricultural University, Ya'an 625014, China
[5]Co-first author
[*]Correspondence: roundtree318@hotmail.com (S.Y.)

SUMMARY

The 2019 novel SARS-like coronavirus (SARS-CoV-2) entry depends on the host membrane serine protease TMPRSS2, which can be blocked by some clinically-proven drugs. Here we analyzed spatial relevance between glycosylation sequons and antibody epitopes and found that, different from SARS-CoV S, most high-surface-accessible epitopes of SARS-CoV-2 S are blocked by the glycosylation, and the optimal epitope with the highest surface accessibility is covered by the S1 cap. TMPRSS2 inhibitor treatments may prevent unmasking of this epitope and therefore prolong virus clearance and may induce antibody-dependent enhancement. Interestingly, a heparin-binding sequence immediately upstream of the S1/S2 cleavage site has been found in SARS-CoV-2 S but not in SARS-CoV S. Binding of SARS-CoV-2 with heparins may lead to exposure of S686, which then facilitates the S1/S2 cleavage, induces exposure of the optimal epitope, and therefore increases the antibody titres. A combination of heparin and vaccine (or convalescent serum) treatments thus is recommended.

Graphical Abstract

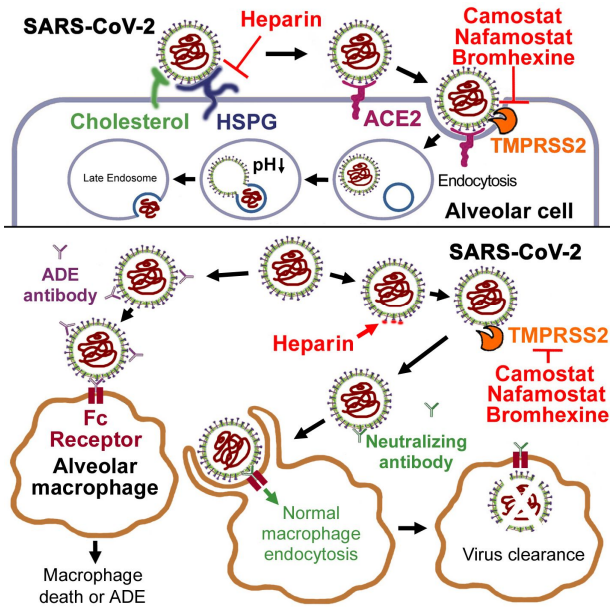

 doi:10.20944/preprints202006.0249.v1

In Brief

Most strong epitopes of SARS-CoV-2 S are blocked by the glycosylation, and the optimal epitope with the highest surface accessibility is covered by the S1 subunit. Heparin facilitates the S1/S2 cleavage. Therefore, TMPRSS2 inhibitors may prolong but heparins may accelerate SARS-CoV-2 clearance.

Highlights

- Most strong epitopes of SARS-CoV-2 S are covered by glycans or the S1 subunit.
- TMPRSS2 inhibitor may prevent unmasking of the optimal epitope.
- Free heparins may induce more exposure of the optimal epitope.
- Max blood concentrations of TMPRSS2 inhibitors are below IC_{90}.

INTRODUCTION

Considering the wide spread of the 2019 novel SARS-like coronavirus (SARS-CoV-2), many candidate drugs have been proposed and testified. No highly-specific anti-viral treatment exists. Therefore, host-directed therapies have been repurposed to treat the novel coronavirus disease 2019 (COVID-19), such as some immunomodulators to prevent the cytokine storm and drugs to inhibit the virus entry or endocytosis (Zumla et al., 2020).

SARS-like coronaviruses utilize angiotensin-converting enzyme 2 (ACE2) as the receptor (Yan et al., 2020). And a plasma membrane serine protease TMPRSS2 is responsible for the proteolysis of viral spike (S) proteins in the post-receptor-binding stage (Glowacka et al., 2011; Kawase et al., 2012; Matsuyama et al., 2010; Shulla et al., 2011; Yamamoto et al., 2016). Viral spike (S) protein S1 attaches the virion to the cell membrane by interacting with the host receptor, initiating the infection. Binding to human ACE2 receptors and internalization of the virus into the endosomes of the host cell induce conformational changes in the S glycoprotein. Proteolysis by TMPRSS2 may unmask the fusion peptide of S2 and activate membranes fusion within endosomes. Spike protein S2 mediates fusion of the virion and cellular membranes by acting as a class I viral fusion protein (Xia et al., 2020). Under the current model, the protein has at least three conformational states: pre-fusion native state, pre-hairpin intermediate state, and post-fusion hairpin state. During viral and target cell membrane fusion, the coiled coil regions (heptad repeats) assume a trimer-of-hairpins structure, positioning the fusion peptide in close proximity to the C-terminal region of the ectodomain. The formation of this structure appears to drive apposition and subsequent fusion of viral and target cell membranes (Xia et al., 2020).

Recently, Hoffmann et al. (2020) found that a TMPRSS2 inhibitor camostat blocked CoV infection in-vitro. Here we analyzed spatial relevance between glycosylation sequons and antibody epitopes and found that, different from SARS-CoV S, most high-surface-accessible epitopes of SARS-CoV-2 S are blocked by the glycosylation, and the optimal epitope with the highest surface accessibility is covered by the S1 cap. TMPRSS2 inhibitor treatments may prevent unmasking of this epitope and therefore prolong virus clearance subsequently. A clinical study suggested that higher TMPRSS2 levels in prostate cancer patients did not increase their illness duration after SARS-CoV-2 infections, but decreased the mortality rate significantly; inhibition to TMPRSS2 (as androgen-deprivation therapy) may not improve the outcomes (Montopoli et al., 2020). Interestingly, a heparin-binding sequence immediately upstream of the S1/S2 cleavage site has been found in SARS-CoV-2 S but not in SARS-CoV S, indicating that free heparins may promote the S1/S2 cleavage, induce exposure of the optimal epitope, and therefore accelerate the virus clearance. This assumption has been proved by a serological study that adding 10 μM heparins into the sera from COVID-19 patients led to a four-fold increase in antibody titres (Perera et al., 2020).

Preprints (www.preprints.org) | NOT PEER-REVIEWED | Posted: 21 June 2020 doi:10.20944/preprints202006.0249.v1

RESULTS AND DISCUSSION

Positive Electrostatic Potential of SARS-CoV-2 S Protein May Explain Its High Affinity to ACE2.

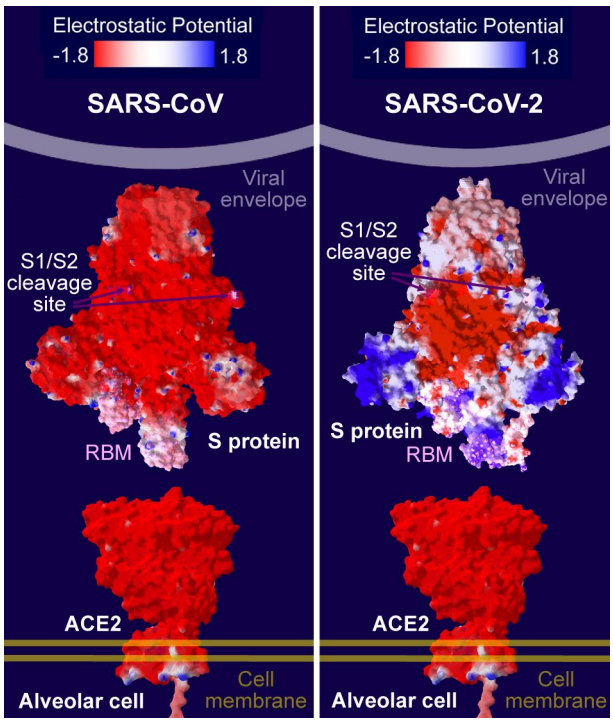

Figure 1. Electrostatic Potential of SARS-CoV S, SARS-CoV-2 S and Human ACE2

The red-to-blue color on the molecular surface indicates the electrostatic potential (red: −1.8; blue: 1.8). The S1/S2 cleavage sites are marked with the dark purple color. The receptor-binding motifs (RBM) are marked with the pale lavender color.

The predominant state of the trimer has one of the three receptor-binding domains (RBDs) rotated up in a receptor-accessible conformation. Biophysical and structural evidences indicated that ACE2 bound to the SARS-CoV-2 S ectodomain with about 15 nM affinity, which is 10 to 20-fold higher than ACE2 binding to SARS-CoV S (Yan et al., 2020). Here we calculated electrostatic potential of SARS-CoV S protein, SARS-CoV-2 S protein and human ACE2 (Figure 1). Interestingly, both SARS-CoV S and ACE2 protein surfaces are uniformly negatively-charged, and therefore they repel each other. However, a large part of SARS-CoV-2 S protein surface is electrically neutral but its receptor-binding motif (RBM) is positive-charged, and therefore SARS-CoV-2 S and ACE2 attract each other. The S1/S2 cleavage sites are distributed in the middle of both SARS-CoV S and SARS-CoV-2 S proteins, implying that TMPRSS2-mediated S1/S2 cleavage may not influence ACE2 binding.

SARS-CoV-2 S Fusion Core Peptides Are More Hydrophobic than SARS-CoV S

A study of the X-ray crystal structure revealed that the six-helical fusion core in the SARS-CoV-2 S protein S2 subunit is formed by interaction between two heptad repeat domains HR1 and HR2 (Xia et al., 2020). The three HR1 domains (894-966 of SARS-CoV S protein or 912-984 of SARS-CoV-2 S protein) form a parallel trimeric coiled-coil center, around which three HR2 domains (1145-1195 of SARS-CoV S protein or 1163-1213 of SARS-CoV-2 S protein) are entwined in an antiparallel manner (Xia et al., 2020). The interaction between these two domains is predominantly a hydrophobic force. Each pair of two adjacent

Preprints (www.preprints.org) | NOT PEER-REVIEWED | Posted: 21 June 2020 doi:10.20944/preprints202006.0249.v1

HR1 helices forms a deep hydrophobic groove, providing the binding site for hydrophobic residues of the HR2 domain. The hydrophobic appearance (electrically neutral surface) plays an important role in the membrane fusion process (Xia et al., 2020).

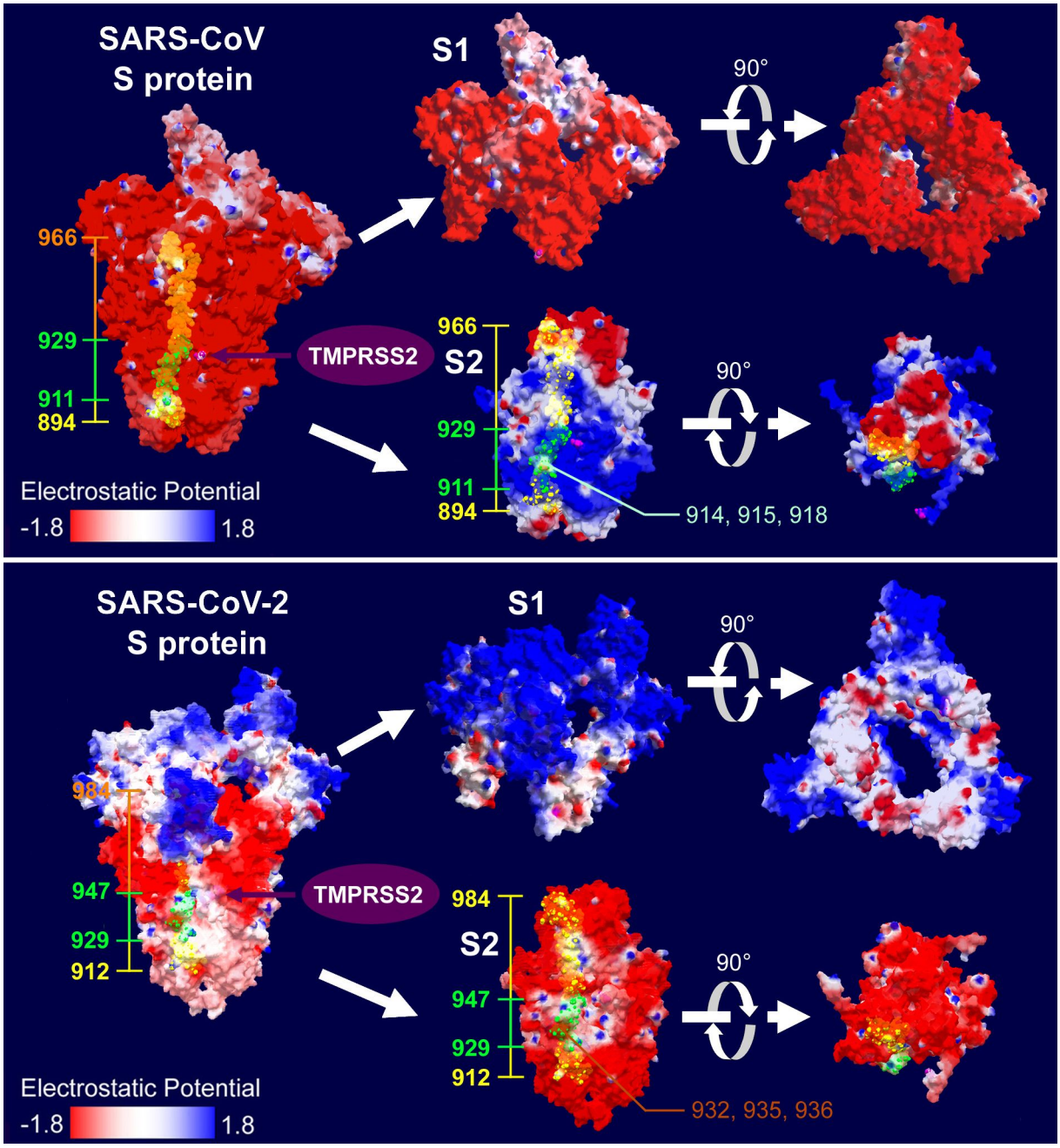

Figure 2. Electrostatic Potential of SARS-CoV and SARS-CoV-2 S1 and S2 Subunits

The Viral spike (S) protein could be divided into S1 and S2 subunits upon the cleavage by TMPRSS2. The red-to-blue color on the molecular surface indicates the electrostatic potential (red: −1.8; blue: 1.8). The S1/S2 cleavage sites are marked with the dark purple color. The heptad repeat domain HR1 on one of the three monomers is marked with orange (invisible segment covered by the S1 cap), green (the fusion core) and yellow colors (visible segment without a cover of S1 cap). In the SARS-CoV fusion core, only three aa distribute on an electrically-neutral area (marked with the pale green color); while the others distribute on the hydrophilic area. Different from SARS-CoV, the SARS-CoV-2 fusion core is much more hydrophobic that only three aa distribute on an electrically-negative area (marked with the brown color) and the others

Preprints (www.preprints.org) | NOT PEER-REVIEWED | Posted: 21 June 2020 doi:10.20944/preprints202006.0249.v1

distribute on the electrically-neutral area.

The SARS-CoV fusion core is composed of 19 amino acids (aa; 911-929 of SARS-CoV S); while the SARS-CoV-2 fusion core is also composed of 19 aa (929-947 of SARS-CoV-2 S; Figure 2). Interestingly, a majority of SARS-CoV fusion core peptide surface is negatively-charged, which could be converted into positive-charged after the TMPRSS2 cleavage, indicating an electrical charge redistribution. Among the 19 aa, only three aa distribute on an electrically-neutral area; while the others distribute on the hydrophilic area. Different from SARS-CoV, the SARS-CoV-2 fusion core is much more hydrophobic that only three aa distribute on an electrically-negative area and the others distribute on the electrically-neutral area. More hydrophobic appearance of SARS-CoV-2 fusion core may be another reason for its higher infectivity compared to SARS-CoV. Interestingly, C-terminus of HR1 domain in either SARS-CoV S (930-966 aa) or SARS-CoV-2 S (948-984 aa) is covered by the S1 subunit, which could be unmasked upon proteolysis by TMPRSS2, also confirming the role of TMPRSS2 in the conformational changes required for the membrane fusion process.

The Optimal Epitope with the Highest Surface Accessibility Is Covered by the S1 Cap

Being exposed on the viral surface, S proteins are a major target for host antibodies and are referred to as viral antigens; these antigens are therefore targets for vaccine development (Zheng and Song, 2020). However, viral envelope proteins are often modified by the attachment of complex glycans. The glycosylation of these surface antigens helps the pathogen evade recognition by the host immune system by cloaking the protein surface from detection by antibodies, and can influence the ability of the host to raise an effective adaptive immune response or even be exploited by the virus to enhance infectivity (Baum and Cobb, 2017; Pereira et al., 2018).

In this study, we computed sequence-based antibody epitopes on spike proteins of SARS-CoV and SARS-CoV-2 (Tables S1 and S2). As the surface accessibility of epitope is the most important determinant to the interaction between antibody and antigen, the possible antibody epitopes were filtered with the surface accessible scores by using the default threshold value of 1.0 (Emini et al., 1985). Then the epitope candidates were re-scored by using BepiPred-2.0 bioinformatic tool with the default threshold value of 0.50 (Jespersen et al., 2017). 27 epitopes were found on SARS-CoV S protein, among which 10 epitopes had been ruled out due to the low epitope scores. And 30 epitopes were identified on SARS-CoV-2 S, among which 9 epitopes had been ruled out due to the low epitope scores (Tables S1 and S2). In SARS-CoV RBD region (306-527) and SARS-CoV-2 RBD region (319-541) respectively, 4 epitopes and 6 epitopes were screened out finally. Our epitope prediction has been proved by two clinical studies. In one study, 399 human monoclonal antibodies (mAbs) have been sorted in 10 SARS-CoV-2 patients, but only 35 S-protein-specific mAbs were acquired, among which, 4 mAbs recognize RBD (Chi et al., 2020). Another study indentified the S230 antibody, which was isolated from memory B cells of a SARS-CoV-infected individual and potently neutralized a broad spectrum of SARS-CoV isolates of human and animal origins (Rockx et al., 2008). The S230 epitope is centered around L443 on S protein and Y408, Y442, F460 and Y475 participate binding to this antibody (Rockx et al., 2008), which matches to a 14 aa epitope candidate (431-444) screened out in this study with a high surface accessibility (SA) score of 3.149 (Table S1).

Preprints (www.preprints.org) | NOT PEER-REVIEWED | Posted: 21 June 2020 doi:10.20944/preprints202006.0249.v1

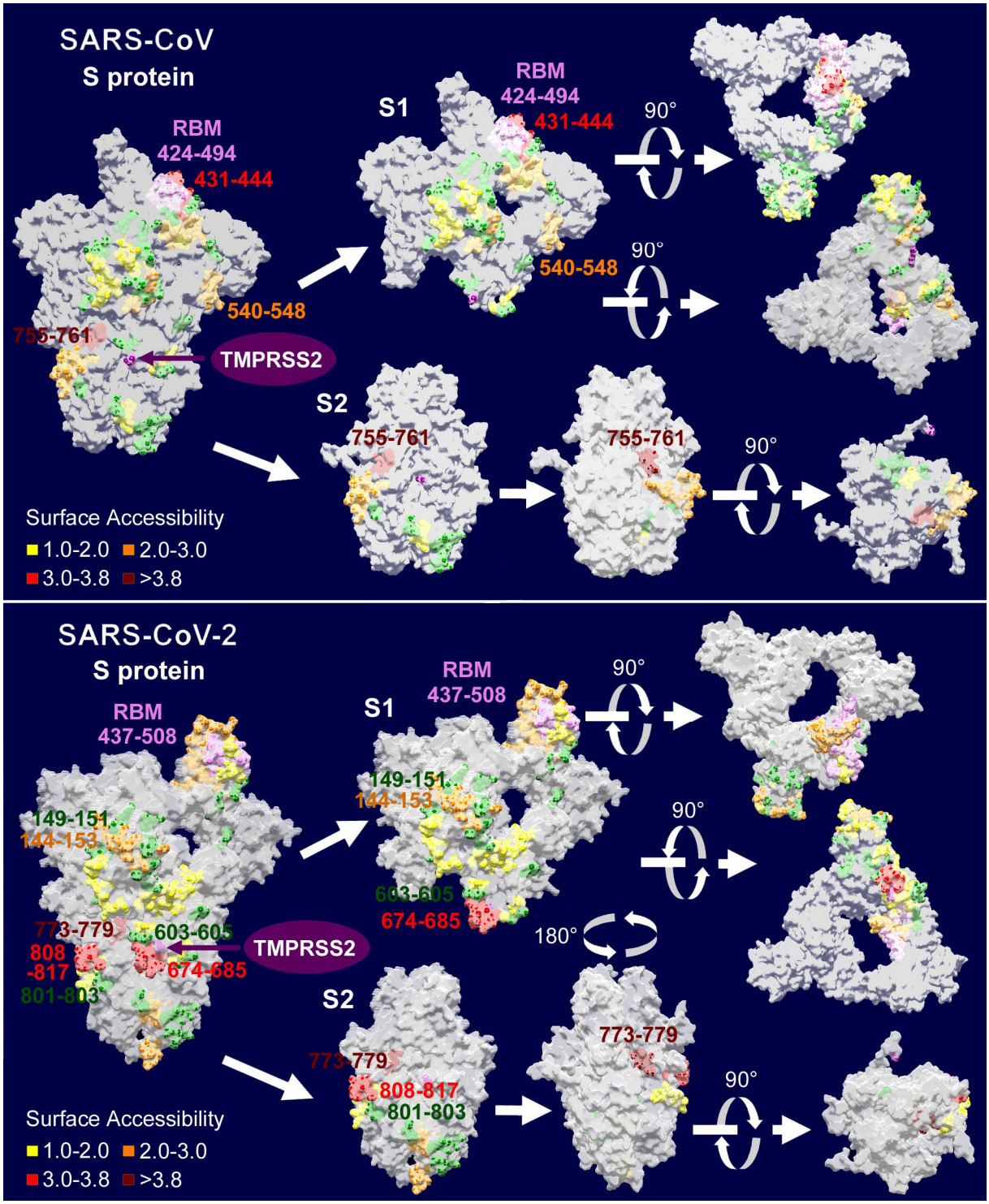

Figure 3. Distribution of Glycosylation Sequons and Antibody Epitopes on SARS-CoV S and SARS-CoV-2 S The Viral spike (S) protein could be divided into S1 and S2 subunits after the cleavage by TMPRSS2. The S1/S2 cleavage sites are marked with the dark purple color. The receptor-binding motifs (RBM) are marked with the pale lavender color. Putative epitopes with different surface accessibilities (SA) are marked with yellow (SA 1.0-2.0), orange (SA 2.0-3.0), red (SA 3.0-3.8) and brown (SA > 3.8) colors. Glycosylation sequons are marked with the green color. The putatively-optimal epitope (755-761) of SARS-CoV with the highest SA score of 4.431 is located on the cutting surface of S2 subunit, which would be uncovered only after TMPRSS2 cleavage. And the putatively-optimal epitope (773-779) of SARS-CoV-2 with the highest SA

Preprints (www.preprints.org) | NOT PEER-REVIEWED | Posted: 21 June 2020 doi:10.20944/preprints202006.0249.v1

score of 4.868 is also located on the cutting surface of S2 subunit, whose binding requires removal of the S1 cap. Due to the coverage limitation in the Swiss model, glycosylation sequons and epitopes in 1120-1255 aa of SARS-CoV S or in 1147-1273 aa of SARS-CoV-2 S are not shown in the figure. To present the sites more clearly, only one of the three monomers is labeled.

Walls et al. (2020) indentified N-linked glycosylation sequons in SARS-CoV S and SARS-CoV-2 S. Along with these data, spatial relevance between glycosylation sequons and antibody epitopes were further analyzed (Figure 3). Grant et al. (2020) demonstrated that most SARS-CoV and SARS-CoV-2 epitopes are shielded by glycans, and only areas of the protein surface at the apex of the S1 domain appear to be accessible to known antibodies (Vankadari and Wilce, 2020). A visual examination of the structures from molecular dynamics simulation also confirmed that the most exposed epitopes comprise the ACE2 receptor site RBD, specifically at the apex region of the RBM domain (Grant et al., 2020). Similar results were also obtained in this study. On SARS-CoV S, only three strong epitopes with SA scores >3.0 have been identified. One epitope (431-444; matching to the S230 epitope as mentioned above) recognizes RBD and is not surrounded by glycosylation sequons. Another epitope (1238-1243) is located in the C-terminal transmembrane domain (Figure S1) and therefore should not be accessible to any antibody. The putatively-optimal epitope (755-761) with the highest SA score of 4.431 is located on the cutting surface of S2 subunit, which could be uncovered only after TMPRSS2 cleavage (Figure 3). Besides, the epitope 540-548 is also not surrounded by glycosylation sequons, however its relatively low SA score (2.396) may suggest a low neutralizing ability (Figure 3 and Figure S2).

Unfortunately, no strong epitopes (SA scores >3.0) is available that recognizes SARS-CoV-2 RBD. This finding is consistent with the fact that only low level of binding of SARS-CoV-2 S to polyclonal rabbit anti-SARS S1 antibodies T62 was detected (Ou et al., 2020). Two strong epitopes are located on SARS-CoV-2 S1 (674-685) and S2 (808-817) subunit surfaces respectively. However both of them are accompanied with glycosylation sequons. Although these two epitopes have large surface areas, their accompanying glycosylation sequons are located on raised areas, and therefore may form the steric hindrance (Figure 3). There is also a strong epitope (1256-1261) located in the C-terminal transmembrane domain (Figure S1). And the putatively-optimal epitope (773-779) with the highest SA score of 4.868 is also located on the cutting surface of S2 subunit, whose binding requires removal of the S1 cap (Figure 3). Notably, a remarkable alterations in the antigenicity was observed in SARS-CoV-2 that no strong RBD-targeting epitopes is available and almost all high-surface-accessible epitopes are blocked by the glycosylation, including the 4A8 epitope sorted recently (matching to a 10 aa epitope 144-153 indentified in this study; Chi et al., 2020). These results might explain why the sera from convalescent SARS-CoV-2 patients exhibited a much weaker neutralizing antibody response compared to SARS-CoV (Hoffmann et al., 2020).

These results also imply that developing of monoclonal antibodies may not be an idea strategy to treat SARS-CoV-2 infections. Alternatively, recombinant virus vector vaccines, DNA vaccines or inactivated virus vaccines may induce strong cellular immunity rather than humoral immunity that produces antibodies (Chandrashekar et al., 2020; Gao et al., 2020; Yu et al., 2020; Zhu et al., 2020).

TMPRSS2 Protease Inhibitors May Prolong SARS-CoV-2 Clearance and Induce Antibody-Dependent Enhancement

Considering that almost all high-surface-accessible epitopes of SARS-CoV-2 are blocked by the glycan shield, people may deduce that the virus should not be cleaned up by the immune system. But that is not

Preprints (www.preprints.org) | NOT PEER-REVIEWED | Posted: 21 June 2020 doi:10.20944/preprints202006.0249.v1

the truth. The epitope on the cutting surface usually have no time to bind with the corresponding antibody, since the membrane fusion occurs immediately following the S1/S2 cleavage. However, free TMPRSS2 makes the antibody binding possible. TMPRSS2 is a secreted protease that is highly expressed in prostate and lung tissues, especially in secretory epithelia (Afar et al., 2001; Lukassen et al., 2020). TMPRSS2 inactive precursor is a 492 residue protein classified as a type II transmembrane protein, with a 70 amino acid N-terminal cytoplasmic domain, followed by a 36 amino acid transmembrane domain (Lucas et al., 2008). Upon sorting to the cytomembrane, the proenzyme would be converted into the active enzyme through limited proteolysis and removal of both the N-terminal segment and the transmembrane domain (Figure S1; Khan and James, 1998; Lucas et al., 2008). Then the active enzymes (C-terminal) may detach from the membrane and be released (secreted) to the extracellular space. As a result, a small part of SARS-CoV-2 S proteins may be cleavaged by free TMPRSS2 before they bind the receptor ACE2 and then the epitope on the cutting surface may have a time to induce a neutralizing antibody response, although maybe in a low efficiency. Clinical data suggested that SARS-CoV-2 can be cleaned up within 17 days (13–22 days; Xu et al., 2020); while the median duration of SARS-CoV RNA detection is 13 days (6–23 days; Hui et al., 2004).

Some TMPRSS2 inhibitors (such as camostat and nafamostat) block the Middle East respiratory syndrome coronavirus (MERS-CoV) or SARS-CoV infection in-vitro (Kawase et al., 2012; Yamamoto et al., 2016). Hoffmann et al. (2020) further indicated that camostat mesylate treatment significantly inhibited SARS-CoV-2 entry into primary human lung cells. However as analyzed above, the optimal epitope with the highest surface accessibility is covered by the S1 cap and thus TMPRSS2 inhibitors may prevent unmasking of this epitope and prolong virus clearance subsequently. Nevertheless, the delay in virus clearance caused by TMPRSS2 inhibitors may not occur in SARS-CoV infections, because that the neutralizing antibody S230 would play a crucial role in the virus clearance (Rockx et al., 2008).

Antibody-dependent enhancement (ADE) of viral entry has been a major concern for epidemiology, vaccine development, and antibody-based drug therapy (Wan et al., 2020). The ADE antibody binds to the surface spike protein of coronaviruses, triggers a conformational change of the spike via receptor functional mimicry (Walls et al., 2019), and mediates viral entry into IgG Fc receptor-expressing cells (like macrophages) and causes cell death (Wan et al., 2020). Critically, patients who eventually died of SARS displayed similarly accumulated pulmonary proinflammatory, absence of wound-healing macrophages, faster neutralizing antibody responses and higher total antibody titer, all of which indicate a certain level of ADE (Cao, 2020; Tetro, 2020; Zhang et al., 2020; Zhao et al., 2020).

Given that TMPRSS2 inhibitors prevent unmasking of the optimal epitope and thus hamper neutralizing antibody activities, these inhibitors may prolong the persistence of ADE. Although TMPRSS2 inhibitors may prevent macrophage death caused by the SARS-CoV-2 entry, they increase the likelihood of viral attachment to the macrophage surface. Alveolar macrophages underwent functional polarization after such viral attachment, demonstrating a proinflammatory characteristic (Liu et al., 2019). On the other hand, viral attachment to the macrophage surface may further enhance the infectivity via macrophage infiltration, which may worsen the lung injury (Li et al., 2020).

These assumptions have been partly proved in prostate cancer patients infected with SARS-CoV-2 (Montopoli et al., 2020). TMPRSS2 is highly expressed in both localized and metastatic prostate cancers and its transcription is regulated by the androgen receptor. Intriguingly, it has been shown that androgen positively regulates TMPRSS2 expression also in non-prostatic tissues, including lung (Stopsack et al., 2020). Montopoli et al. (2020) indicated that 27.2% (31/114) of prostate cancer COVID-19 male patients without androgen-deprivation therapy developed severe diseases and 15.8% (18/114) died; 28.5% (89/312) of male

Preprints (www.preprints.org) | NOT PEER-REVIEWED | Posted: 21 June 2020 doi:10.20944/preprints202006.0249.v1

patients with other tumors and SARS-CoV-2 developed severe diseases and 18.3% (57/312) died; while among male patients without cancer 10.0% (411/4102) developed severe diseases and 5.8% (237/4102) died. Although only four prostate cancer patients receiving androgen-deprivation therapy were infected with SARS-CoV-2, one patient (1/4) still developed severe diseases. These clinical data imply that higher TMPRSS2 levels in prostate cancer patients did not increase their illness duration, but decreased the mortality rate significantly; inhibition to TMPRSS2 (as androgen-deprivation therapy) may not improve the outcomes.

Nevertheless, only 4 of 5273 (0.076%) prostate cancer patients receiving androgen-deprivation therapy were infected with SARS-CoV-2; while 114 of 37,161 (0.307%) prostate cancer patients without androgen-deprivation therapy were infected with SARS-CoV-2. The infection rate decreased by 75.1% after the androgen-deprivation therapy. Camostat, nafamostat, or other TMPRSS2 inhibitors (e.g. bromhexine as recommended by Stopsack et al., 2020) may be used as prophylactic drugs to reduce the risk of infection, because that TMPRSS2 inhibitors may decrease the initial viral load during the incubation period. However they may be inefficient for the patients who already develop symptoms, or even have a detrimental effect on the virus clearance.

Heparin May Accelerate SARS-CoV-2 Clearance by Facilitating S1/S2 Cleavage

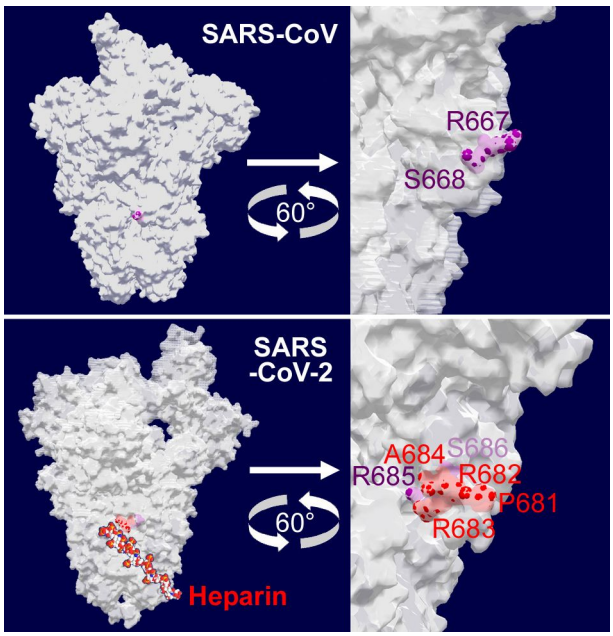

Figure 4. Distribution of a Heparin-Binding Sequence Immediately Upstream of the S1/S2 Cleavage Site on SARS-CoV-2 S But Not on SARS-CoV S

A heparin-binding sequence immediately upstream of the S1/S2 cleavage site has been found in SARS-CoV-2 S but not in SARS-CoV S. The heparin-binding sequence is marked with the red color. Both R667 and S668 in SARS-CoV S cleavage site are exposed on the protein surface (marked with the dark purple color). Contrastingly, although R685 in SARS-CoV-2 S cleavage site is exposed on the protein surface (marked with the dark purple color), S686 in SARS-CoV-2 S is embedded under the protein surface (marked with the light purple color), which may be exposed above the protein surface via a conformational change induced by the heparin binding. To present the sites more clearly, only one of the three monomers is labeled.

Preprints (www.preprints.org) | NOT PEER-REVIEWED | Posted: 21 June 2020 doi:10.20944/preprints202006.0249.v1

Heparin is a mucopolysaccharide sulfuric acid ester that is found especially in the liver and lungs. Heparin is an attractive target for viral adhesion because of its physiological location on the surface of most animal cells, where the initial interactions with viruses occur (de Haan et al., 2005). Previous studies found the heparan sulfate (HS) binding in the S1/S2 cleavage motif of murine coronaviruses (de Haan et al., 2005; Watanabe et al., 2007). Although heparin is not a direct entry receptor for some murine coronaviruses, it induces a conformational change of S1 subunit, which may facilitate the virus entry (Mycroft-West et al., 2020). Here we searched putative HS-binding consensus sequences (XBBXBX, XBXBBX or XBXXBBBX; X=any amino acid, B=basic amino acid; de Haan et al., 2005; Watanabe et al., 2007) on both SARS-CoV S and SARS-CoV-2 S, and interestingly found that only SARS-CoV-2 S has a HS-binding sequence (681-686 PRRARS) immediately upstream of the S1/S2 cleavage site (R685-S686; Figure 4). Another intriguing difference between SARS-CoV S and SARS-CoV-2 S is that both R667 and S668 in SARS-CoV S cleavage site are exposed on the protein surface, but S686 in SARS-CoV-2 S is embedded under the protein surface (Figure 4). These findings imply that heparin binding may be required for SARS-CoV-2 S1/S2 cleavage, but not for SARS-CoV S1/S2 cleavage. Binding of SARS-CoV-2 with membrane-bound heparins may lead to exposure of S686 by a conformational change, which then facilitates the S1/S2 cleavage and the subsequent membrane fusion (virus entry). While if SARS-CoV-2 S binds free heparins in the interstitial fluids or in the blood, the enhanced S1/S2 cleavage may induce more exposure of the optimal epitope 773-779, which therefore accelerates SARS-CoV-2 clearance (Figure 5). One copy of the HS-binding motif adjacent to the cleavage site in the S protein is a common characteristic of murine coronaviruses (de Haan et al., 2005; Watanabe et al., 2007), which suggests that one or more rodent species might be the intermediate hosts of SARS-CoV-2 where the virus was once circulating and mutating (Yuan et al., 2020a).

The enhancement to antigenicity by free heparins has been confirmed by a serological assay (Perera et al., 2020). They observed a 1.0–1.5 $\log_{10}$ reduction in $TCID_{50}$ (median tissue culture infective dose) when the SARS-CoV-2 was diluted in the heparin medium compared with the control medium. They also carried out titrations of three sera (from COVID-19 patients) with known micro-neutralisation antibody titres of 1:40, 1:80 and 1:80, with the serum dilutions carried out in parallel in heparin medium or the control medium without heparin. The antibody titres in the sera diluted in the heparin medium were 1:160, 1:320 and 1:320 respectively (Perera et al., 2020). These results suggested that heparin (heparinised plasma usually contains about 10 μM heparins) may induce a four-fold increase in the antibody titres against SARS-CoV-2. A combination of heparin and vaccine (or convalescent serum) treatments may help to enhance the efficiency of the antibodies.

Besides above mechanism, free heparins may also inhibit coronavirus entry by preventing viral adhesion on the cell surface. SARS-CoV rolls onto the cell membrane by binding to cell-surface cholesterols (Wang et al., 2008) and heparan sulfate proteoglycans (HSPGs; Lang et al., 2011) and scans for the specific entry receptor ACE2, which leads to subsequent cell entry (Figure 5). Methyl-β-cyclodextrin (MβCD), an oligosaccharide used to deplete cholesterols from cell membranes was shown to inhibit SARS-CoV entry in a dose-dependent manner (although the 90% inhibitory concentration IC_{90} was as high as 10 mM; Wang et al., 2008). Similarly, heparin treatments inhibited SARS-pseudovirus adhesion on the cell surface in a dose-dependent manner with a IC_{90} of about 20 μM (Lang et al., 2011). According to above analysis of spatial relevance between the heparin-binding sequence and the S1/S2 cleavage site on SARS-CoV-2 S, a much lower IC_{90} specific to SARS-CoV-2 could be expected.

The therapeutic effects of heparins on SARS-CoV-2 infections have been confirmed clinically. Anticoagulant therapy with low molecular weight heparin (LMWH) has been suggested to treat COVID-19, because that the severe patients have the risk of disseminated intravascular coagulation and venous

Preprints (www.preprints.org) | NOT PEER-REVIEWED | Posted: 21 June 2020 doi:10.20944/preprints202006.0249.v1

thromboembolism (Ahmed and Anirvan, 2020; Lin et al., 2020; Tang et al., 2020; Yin et al., 2020). Moreover, heparin also showed a good therapeutic effect to acute respiratory distress syndrome (ARDS), which is a common complication of viral pneumonia (Thompson et al., 2017). Here we added an important information that heparin may also inhibit SARS-CoV-2 entry by both enhancing neutralizing antibody titres and preventing viral adhesion on the cell surface. Thus, LMWH anticoagulant therapy may also work for the non-severe patients. On the other hand, COVID-19 has a prominent feature, that is, a large amount of mucus (oedema and plasma exudation) could be found in the small airway, and it may eventually block the airway, which may be an important reason for the high mortality after later mechanical ventilation and high-flow oxygen inhalation (Barton et al., 2020). Therefore, nebulized heparin, oxygen supply or other inhalation therapies should be given at the early stages of COVID-19 (Yuan et al., 2020b).

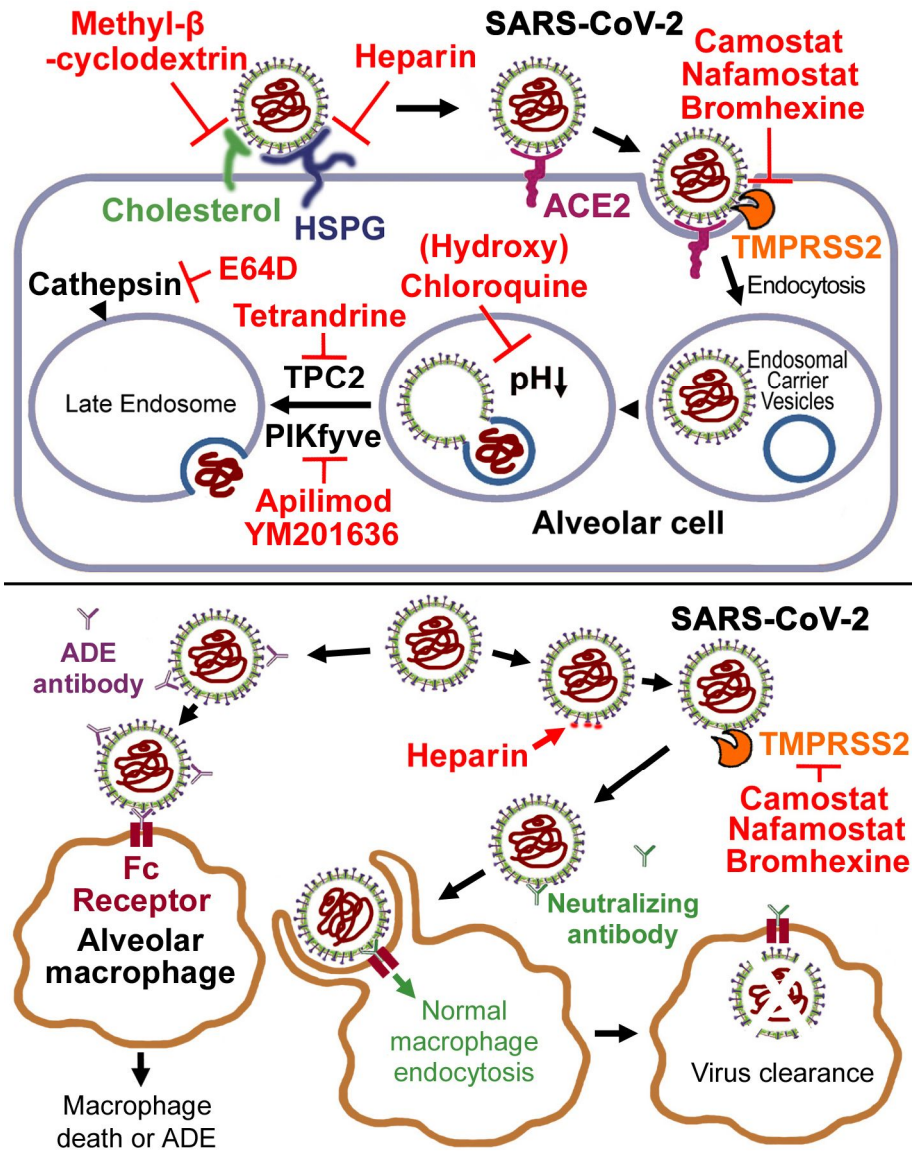

Figure 5. Drugs against SARS-CoV-2 Entry and Their Effects on the Virus Clearance

Coronavirus rolls onto the cell membrane by binding to cell-surface cholesterols and heparan sulfate proteoglycans (HSPGs) and scans for the specific entry receptor ACE2, which leads to subsequent cell entry. Camostat, nafamostat or bromhexine inhibits the plasma membrane protease TMPRSS2, which is responsible for the proteolysis of viral S proteins in the post-receptor-binding stage. Methyl-β-cyclodextrin and heparin inhibit virus binding with cholesterols and HSPGs respectively. Chloroquine neutralizes acidic

Preprints (www.preprints.org) | NOT PEER-REVIEWED | Posted: 21 June 2020 doi:10.20944/preprints202006.0249.v1

pH in the endosome, which is necessary for viral nucleocapsid release into the cytoplasm. PIKfyve inhibitors apilimod and YM201636, TPC2 inhibitor tetrandrine and cathepsin L inhibitors E64D and SID 26681509 prevent the virus entry. On the other hand, in the interstitial fluids or in the blood, free heparin binding may lead to exposure of the S1/S2 cleavage site by a conformational change. Then the enhanced S1/S2 cleavage by free TMPRSS2 may induce more exposure of the optimal epitope 773-779, which therefore accelerates neutralizing-antibody-mediated SARS-CoV-2 clearance. Contrastingly, TMPRSS2 inhibitors prevent unmasking of the optimal epitope and thus hamper neutralizing antibody activities, prolonging the virus clearance. Although TMPRSS2 inhibitors may prevent macrophage death caused by the SARS-CoV-2 entry, they increase the likelihood of viral attachment to the macrophage surface, which induces proinflammatory responses and antibody-dependent enhancement (ADE).

All FDA-Approved TMPRSS2 Inhibitors Would Not Achieve the Effective Concentrations, But Nebulized Heparin Would Achieve a Local High Concentration

IC_{50} and IC_{90} of camostat against either SARS-CoV or SARS-CoV-2 were about 1 μM and 5 μM respectively (Hoffmann et al., 2020). Although no direct study about nafamostat against SARS-CoV or SARS-CoV-2 is available, two previous studies showed that IC_{50} of nafamostat was about 10 times lower than that of camostat against MERS-CoV (Shirato et al., 2013; Yamamoto et al., 2016). Thus, it can be deduced that IC_{50} and IC_{90} of nafamostat against either SARS-CoV or SARS-CoV-2 may be 0.1 μM and 0.5 μM respectively. However the maximum blood concentration of camostat at the normal oral dose of 100 mg would achieve only 0.21 μM (Midgley et al., 1994); while the maximum blood concentration of nafamostat injection at the maximum dose of 40 mg would achieve only 0.27 μM (Iwama et al., 1998). Similarly, the maximum blood concentration of bromhexine at the maximum dose (single oral dose of 32 mg) would achieve only 0.36 μM (Bechgaard and Nielsen, 1982); while IC_{90} of bromhexine on TMPRSS2 activity is about 1 μM (Lucas et al., 2014). In summary, all FDA-approved TMPRSS2 inhibitors would not achieve the effective blood concentrations. Thus they may neither inhibit SARS-CoV-2 entry, nor reduce the risk of infection efficiently. More effective TMPRSS2 inhibitors still need to be developed.

Contrastingly, nebulized heparin is inhaled directly into the lung, so it can reach a local high concentration in alveolar cells. Although the alveolar concentration cannot be easily estimated (1 mg/mL LMWH is usually used for the ultrasonic atomization, which is equal to about 67 μM), it may be higher than 10 μM that can induce a 1.0–1.5 $\log_{10}$ reduction in $TCID_{50}$ of SARS-CoV-2 (Perera et al., 2020). Nevertheless, given that heparin may cause thrombocytopenia and thrombosis, more clinical trials are still required to determine the optimal dosage and therapeutic time.

Besides TMPRSS2 inhibitors and heparins, other drugs that inhibit coronavirus entry are summarized and listed in Table 1 and Figure 5. The cellular alkalizers also repress virus entry through neutralizing acidic pH in the early endosomes, which is necessary for viral nucleocapsid release into the cytoplasm. Chloroquine and its derivative hydroxychloroquine are such alkalizers and are used clinically as antimalarial medicines. In-vitro experiments confirmed that chloroquine is highly effective in the control of SARS-CoV-2 infection (the inhibition ratio of 10 μM chloroquine could reach over 90%; Liu et al., 2020; Wang et al., 2020; Yao et al., 2020). And a recent clinical trial showed that hydroxychloroquine treatment is significantly associated with viral load reduction and remission of symptoms in COVID-19 patients (Gautret et al., 2020). However chloroquine did not reduce the duration of Dengue virus type 2 infection in a human clinical trial and showed several adverse effects, primarily vomiting (Tricou et al., 2010). And the high-dosage chloroquine may not reduce the mortality rate but cause more instance of QTc interval greater than 500 milliseconds, showing a cardiac toxicity (Borba et al., 2020). More rigorous clinical trials

Preprints (www.preprints.org) | NOT PEER-REVIEWED | Posted: 21 June 2020 doi:10.20944/preprints202006.0249.v1

on SARS-CoV-2 are still required.

Table 1. Drugs against SARS-CoV-2 Entry, Their IC_{90} and the Demerits

Drug's name	Mechanisms	IC_{90} to SARS-CoV	IC_{90} to SARS-CoV-2	Demerits
Camostat	TMPRSS2 inhibitor	5 μM	5 μM	Max plasma concentration < 0.27 μM and may causing a prolonged virus clearance
Nafamostat		0.5 μM*	0.5 μM*	
Bromhexine		1 μM to TMPRSS2		Max plasma concentration < 0.36 μM and may causing a prolonged virus clearance
Methyl-β -cyclodextrin	Cholesterol depletion	10 mM	N.A.	Non-FDA-approved drug with a very high IC_{90}
Heparin	Cell surface binding inhibitor	20 μM	< 10 μM†	Thrombocytopenia and thrombosis
Chloroquine	Alkalizer in the endosome	N.A.	100 μM	non-decreased mortality rate with side effects
Hydroxy -chloroquine		N.A.	10 μM	
Apilimod	PIKfyve inhibitor	100 nM	100 nM	Non-FDA-approved drug with side effects
YM201636		N.A.	10 μM	Non-FDA-approved drug with side effects
Tetrandrine	TPC2 inhibitor	N.A.	3 μg/ml	Non-FDA-approved drug with side effects
E64D	Cathepsin L inhibitor	N.A.	2 μM	Non-FDA-approved drug with side effects
SID 26681509		N.A.	30 μM	Non-FDA-approved drug with side effects

*Although no direct study about nafamostat on SARS-CoV or SARS-CoV-2 is available, two previous studies showed that IC_{50} of nafamostat was about 10 times lower than that of camostat against MERS-CoV. Thus, it could be deduced that IC_{90} of nafamostat against either SARS-CoV or SARS-CoV-2 may be 0.5 μM. †10 μM heparins induced a 1.0–1.5 log_{10} reduction in $TCID_{50}$ of SARS-CoV-2. Thus, it could be deduced that IC_{90} of heparin against SARS-CoV-2 may be < 10 μM. N.A., Not Available.

SARS-like coronavirus entry was mediated by a clathrin- and caveolae-independent mechanism (Wang et al., 2008). Drugs against clathrin-mediated endocytosis (e.g. chlorpromazine) or caveolae-dependent endocytosis (e.g. filipin and nystatin) had no inhibitory effects on the virus entry (Wang et al., 2008). The clathrin-pathway inhibitor baricitinib (Richardson et al., 2020; Stebbing et al., 2020) may not work as well. Nevertheless, a recent study demonstrated that phosphatidylinositol 3-phosphate 5-kinase (PIKfyve), two pore channel subtype 2 (TPC2), and cathepsin L are critical for SARS-CoV-2 entry (Ou et al., 2020), and PIKfyve inhibitors apilimod and YM201636, TPC2 inhibitor tetrandrine and cathepsin L inhibitors E64D and SID 26681509 prevent the virus entry (Table 1; Ou et al., 2020). However, none of them are FDA-approved drug and may have many side effects. In a nutshell, among all FDA-approved drugs against SARS-CoV-2 entry putatively, camostat, nafamostat or bromhexine may be candidate prophylactic drugs, nebulized heparin may be a promising therapeutic drug, and validity and safety of (hydroxy)chloroquine require further clinical investigations.

STAR+METHODS

Detailed methods are provided in the online version of this paper and include the following:

- KEY RESOURCES TABLE
- LEAD CONTACT AND MATERIALS AVAILABILITY
- METHOD DETAILS
  - Homology modeling of ACE2 and viral spike proteins
  - Analysis of antibody epitopes
  - Prediction of transmembrane domain
  - Alignment of SARS-CoV and SARS-CoV-2 spike proteins
- QUANTIFICATION AND STATISTICAL ANALYSIS
- DATA AND CODE AVAILABILITY

ACKNOWLEDGMENTS

This work was supported by the Supporting Program of Sichuan Agricultural University to S.Y.

AUTHOR CONTRIBUTIONS

Conceptualization, S.Y.; Formal analysis, S.Y., S.C.J., Z.W.Z. and Z.L.L.; Investigation, C.Q.W., M.Y., Y.E.C., Q.T., T.L., X.Y.T., G.D.C and Z.J.; Writing – Original Draft, S.Y.; Writing – Review & Editing, all authors; Funding acquisition, S.Y.

DECLARATION OF INTERESTS

The authors declare no competing interests.

REFERENCES

Afar, D. E., Vivanco, I., Hubert, R. S., Kuo, J., Chen, E., Saffran, D. C., Raitano, A. B., and Jakobovits, A. (2001). Catalytic cleavage of the androgen-regulated TMPRSS2 protease results in its secretion by prostate and prostate cancer epithelia. Cancer Res. *61*, 1686–1692.

Ahmed, S., and Anirvan, P. (2020). Reply to Rheumatologists' perspective on coronavirus disease 19: is heparin the dark horse for COVID-19?. Clin. Rheumatol. DOI: 10.1007/s10067-020-05145-w.

Barton, L. M., Duval, E. J., Stroberg, E., Ghosh, S., and Mukhopadhyay, S. (2020). COVID-19 Autopsies, Oklahoma, USA. Am. J. Clin. Pathol. *153*, 725–733.

Baum, L. G., and Cobb, B. A. (2017). The direct and indirect effects of glycans on immune function. Glycobiology *27*, 619–624.

Bechgaard, E., and Nielsen, A. (1982). Bioavailability of bromhexine tablets and preliminary pharmacokinetics in humans. Biopharm. Drug Dispos. *3*, 337–344.

Bertoni, M., Kiefer, F., Biasini, M., Bordoli, L., and Schwede, T. (2017). Modeling protein quaternary structure of homo- and hetero-oligomers beyond binary interactions by homology. Sci. Rep. 7, 10480.

Biasini, M., Bienert, S., Waterhouse, A., Arnold, K., Studer, G., Schmidt, T., Kiefer, F., Gallo Cassarino, T., Bertoni, M., Bordoli, L., et al. (2014). SWISS-MODEL: modelling protein tertiary and quaternary structure using evolutionary information. Nucleic Acids Res. *42*, W252–W258.

Bienert, S., Waterhouse, A., de Beer, T. A. P., Tauriello, G., Studer, G., Bordoli, L., and Schwede, T. (2017). The SWISS-MODEL Repository - new features and functionality. Nucleic Acids Res. 45, D313–D319.

Borba, M. G. S., Val, F., Sampaio, V. S., Alexandre, M., Melo, G. C., Brito, M., Mourão, M., Brito-Sousa, J. D., Baía-da-Silva, D., Guerra, M., et al. (2020). Effect of high vs low doses of chloroquine diphosphate as

adjunctive therapy for patients hospitalized with severe acute respiratory syndrome coronavirus 2 (SARS-CoV-2) infection: a randomized clinical trial. JAMA Network Open *3*, e208857.

Cao, X. (2020). COVID-19: immunopathology and its implications for therapy[J]. Nat. Rev. Immunol. *20*, 269–270.

Chandrashekar, A., Liu, J., Martinot, A. J., McMahan, K., Mercado, N. B., Peter, L., Tostanoski, L. H., Yu, J., Maliga, Z., Nekorchuk, M., et al. (2020). SARS-CoV-2 infection protects against rechallenge in rhesus macaques. Science DOI: 10.1126/science.abc4776.

Chi, X., Yan, R., Zhang, J., Zhang, G., Zhang, Y., Hao, M., Zhang, Z., Fan, P., Dong, Y., Yang, Y., et al. (2020). A potent neutralizing human antibody reveals the N-terminal domain of the Spike protein of SARS-CoV-2 as a site of vulnerability. bioRxiv DOI: 10.1101/2020.05.08.083964.

de Haan, C. A., Li, Z., te Lintelo, E., Bosch, B. J., Haijema, B. J., and Rottier, P. J. (2005). Murine coronavirus with an extended host range uses heparan sulfate as an entry receptor. J. Virol. *79*, 14451–14456.

Emini, E. A., Hughes, J. V., Perlow, D. S., and Boger, J. (1985). Induction of hepatitis A virusneutralizing antibody by a virus-specific synthetic peptide. J. Virol. *55*, 836–839.

Forster, P., Forster, L., Renfrew, C., and Forster, M. (2020). Phylogenetic network analysis of SARS-CoV-2 genomes. Proc. Natl. Acad. Sci. USA *117*, 9241–9243.

Gao, Q., Bao, L., Mao, H., Wang, L., Xu, K., Yang, M., Li, Y., Zhu, L., Wang, N., Lv, Z., et al. Development of an inactivated vaccine candidate for SARS-CoV-2. Science DOI: 10.1126/science.abc1932.

Gautret, P., Lagier, J. C., Parola, P., Hoang, V. T., Meddeb, L., Mailhe, M., Doudier, B., Courjon, J., Giordanengo, V., Vieira, V. E., et al. (2020). Hydroxychloroquine and azithromycin as a treatment of COVID-19: results of an open-label non-randomized clinical trial. Int. J. Antimicrob. Agents DOI: 10.1016/j.ijantimicag.2020.105949.

Glowacka, I., Bertram, S., Müller, M. A., Allen, P., Soilleux, E., Pfefferle, S., Steffen, I., Tsegaye, T. S., He, Y., Gnirss, K., et al. (2011). Evidence that TMPRSS2 activates the severe acute respiratory syndrome coronavirus spike protein for membrane fusion and reduces viral control by the humoral immune response. J. Virol. *85*, 4122–4134.

Grant, O. C., Montgomery, D., Ito, K., and Woods, R. J. (2020). 3D Models of glycosylated SARS-CoV-2 spike protein suggest challenges and opportunities for vaccine development. bioRxiv DOI: 10.1101/2020.04.07.030445.

Hoffmann, M., Kleine-Weber, H., Schroeder, S., Krüger, N., Herrler, T., Erichsen, S., Schiergens, T. S., Herrler, G., Wu, N. H., Nitsche, A., et al. (2020). SARS-CoV-2 cell entry depends on ACE2 and TMPRSS2 and is blocked by a clinically proven protease inhibitor. Cell *181*, 271–280.

Hui, D. S., Chan, M. C., Wu, A. K., and Ng, P. C. (2004). Severe acute respiratory syndrome (SARS): epidemiology and clinical features. Postgrad. Med. J. *80*, 373–381.

Iwama, H., Nakane, M., Ohmori, S., Kaneko, T., Kato, M., Watanabe, K., and Okuaki, A. (1998). Nafamostat mesilate, a kallikrein inhibitor, prevents pain on injection with propofol. Br. J. Anaesth. *81*, 963–964.

Jespersen, M. C., Peters, B., Nielsen, M., and Marcatili, P. (2017). BepiPred-2.0: improving sequence-based B-cell epitope prediction using conformational epitopes. Nucleic Acids Res. *45*, W24–W29.

Kawase, M., Shirato, K., van der Hoek, L., Taguchi, F., and Matsuyama, S. (2012). Simultaneous treatment of human bronchial epithelial cells with serine and cysteine protease inhibitors prevents severe acute respiratory syndrome coronavirus entry. J. Virol. *86*, 6537–6545.

Khan, A. R., and James, M. N. (1998). Molecular mechanisms for the conversion of zymogens to active proteolytic enzymes. Protein Sci. *7*, 815–836.

Krogh, A., Larsson, B., von Heijne, G., and Sonnhammer, E. L. L. (2001). Predicting transmembrane protein

topology with a hidden Markov model: Application to complete genomes. J. Mol. Biol. *305*, 567–580.

Lang, J., Yang, N., Deng, J., Liu, K., Yang, P., Zhang, G., and Jiang, C. (2011). Inhibition of SARS pseudovirus cell entry by lactoferrin binding to heparan sulfate proteoglycans. PLoS One *6*, e23710.

Larkin, M. A., Blackshields, G., Brown, N. P., Chenna, R., McGettigan, P. A., McWilliam, H., Valentin, F., Wallace, I. M., Wilm, A., Lopez, R., et al. (2007). Clustal W and Clustal X version 2.0. Bioinformatics *23*, 2947–2948.

Li, H., Liu, L., Zhang, D., Xu, J., Dai, H., Tang, N., Su, X., and Cao, B. (2020). SARS-CoV-2 and viral sepsis: observations and hypotheses. Lancet *395*, 9–15.

Lin, L., Lu, L., Cao, W., and Li, T. (2020). Hypothesis for potential pathogenesis of SARS-CoV-2 infection-a review of immune changes in patients with viral pneumonia. Emerg. Microbes Infect. *9*, 727–732.

Liu, L., Wei, Q., Lin, Q., Fang, J., Wang, H., Kwok, H., Tang, H., Nishiura, K., Peng, J., Tan, Z., et al. (2019). Anti-spike IgG causes severe acute lung injury by skewing macrophage responses during acute SARS-CoV infection. JCI insight *4*, e123158.

Liu, J., Cao, R., Xu, M., Wang, X., Zhang, H., Hu, H., Li, Y., Hu, Z., Zhong, W., and Wang, M. (2020). Hydroxychloroquine, a less toxic derivative of chloroquine, is effective in inhibiting SARS-CoV-2 infection in vitro. Cell Discov. *6*, 16.

Lucas, J. M., True, L., Hawley, S., Matsumura, M., Morrissey, C., Vessella, R., and Nelson, P. S. (2008). The androgen-regulated type II serine protease TMPRSS2 is differentially expressed and mislocalized in prostate adenocarcinoma. J. Pathol. *215*, 118–125.

Lucas, J. M., Heinlein, C., Kim, T., Hernandez, S. A., Malik, M. S., True, L. D., Morrissey, C., Corey, E., Montgomery, B., Mostaghel, E., et al. (2014). The androgen-regulated protease TMPRSS2 activates a proteolytic cascade involving components of the tumor microenvironment and promotes prostate cancer metastasis. Cancer Discov. *4*, 1310–1325.

Lukassen, S., Chua, R. L., Trefzer, T., Kahn, N. C., Schneider, M. A., Muley, T., Winter, H., Meister, M., Veith, C., Boots, A. W., et al. (2020). SARS-CoV-2 receptor ACE2 and TMPRSS2 are primarily expressed in bronchial transient secretory cells. EMBO J. *39*, e105114.

Matsuyama, S., Nagata, N., Shirato, K., Kawase, M., Takeda, M., and Taguchi, F. (2010). Efficient activation of the severe acute respiratory syndrome coronavirus spike protein by the transmembrane protease TMPRSS2. J. Virol. *84*, 12658–12664.

Midgley, I., Hood, A. J., Proctor, P., Chasseaud, L. F., Irons, S. R., Cheng, K. N., Brindley, C. J., and Bonn, R. (1994). Metabolic fate of 14C-camostat mesylate in man, rat and dog after intravenous administration. Xenobiotica *24*, 79–92.

Moller, S., Croning, M. D. R., and Apweiler. R. (2001). Evaluation of methods for the prediction of membrane spanning regions. Bioinformatics *17*, 646-653.

Montopoli, M., Zumerle, S., Vettor, R., Rugge, M., Zorzi, M., Catapano, C. V., Carbone, G. M., Cavalli, A., Pagano, F., Ragazzi, E., et al. (2020). Androgen-deprivation therapies for prostate cancer and risk of infection by SARSCoV-2: a population-based study (n=4532). Ann. Oncol. DOI: 10.1016/j.annonc.2020.04.479.

Mycroft-West, C., Su, D., Elli, S., Li, Y., Guimond, S., Miller, G., Turnbull, J., Yates, E., Guerrini, M., Fernig, D., et al. (2020). The 2019 coronavirus (SARS-CoV-2) surface protein (Spike) S1 Receptor Binding Domain undergoes conformational change upon heparin binding. bioRxiv DOI: 10.1101/2020.02.29.971093.

Ou, X., Liu, Y., Lei, X., Li, P., Mi, D., Ren, L., Guo, L., Guo, R., Chen, T., Hu, J., et al. (2020). Characterization of spike glycoprotein of SARS-CoV-2 on virus entry and its immune cross-reactivity with SARS-CoV. Nat. Commun. *11*, 1620.

Pereira, M. S., Alves, I., Vicente, M., Campar, A., Silva, M. C., Padrão, N. A., Pinto, V., Fernandes, Â., Dias, A. M., and Pinho, S. S. (2018). Glycans as key checkpoints of T cell activity and function. Front. Immunol. *9*, 2754.

Perera, R. A., Mok, C. K., Tsang, O. T., Lv, H., Ko, R. L., Wu, N. C., Yuan, M., Leung, W. S., Chan, J. M., Chik, T. S., et al. (2020). Serological assays for severe acute respiratory syndrome coronavirus 2 (SARS-CoV-2), March 2020. Euro Surveill. *25*, 2000421.

Richardson, P., Griffin, I., Tucker, C., Smith, D., Oechsle, O., Phelan, A., and Stebbing, J. (2020). Baricitinib as potential treatment for 2019-nCoV acute respiratory disease. Lancet *395*, e30–e31.

Rockx, B., Corti, D., Donaldson, E., Sheahan, T., Stadler, K., Lanzavecchia, A., and Baric, R. (2008). Structural basis for potent cross-neutralizing human monoclonal antibody protection against lethal human and zoonotic severe acute respiratory syndrome coronavirus challenge. J. Virol. *82*, 3220–3235.

Shirato, K., Kawase, M., and Matsuyama, S. (2013). Middle East respiratory syndrome coronavirus infection mediated by the transmembrane serine protease TMPRSS2. J. Virol. *87*, 12552–12561.

Shulla, A., Heald-Sargent, T., Subramanya, G., Zhao, J., Perlman, S., and Gallagher, T. (2011). A transmembrane serine protease is linked to the severe acute respiratory syndrome coronavirus receptor and activates virus entry. J. Virol. *85*, 873–882.

Stebbing, J., Phelan, A., Griffin, I., Tucker, C., Oechsle, O., Smith, D., and Richardson, P. (2020). COVID-19: combining antiviral and anti-inflammatory treatments. Lancet Infect. Dis. *20*, 400–402.

Stopsack, K. H., Mucci, L. A., Antonarakis, E. S., Nelson, P. S., and Kantoff, P. W. (2020). *TMPRSS2* and COVID-19: serendipity or opportunity for intervention? Cancer Discov. DOI: 10.1158/2159-8290.CD-20-0451.

Tang, N., Bai, H., Chen, X., Gong, J., Li, D., and Sun, Z. (2020). Anticoagulant treatment is associated with decreased mortality in severe coronavirus disease 2019 patients with coagulopathy. J. Thromb. Haemost. *18*, 1094–1099.

Tetro J. A. (2020). Is COVID-19 receiving ADE from other coronaviruses? Microb. Infect. *22*, 72–73.

Thompson, B.T., Chambers, R.C., and Liu, K.D. (2017). Acute respiratory distress syndrome. N. Engl. J. Med. *377*, 562–572.

Tricou, V., Minh, N. N., Van, T. P., Lee, S. J., Farrar, J., Wills, B., Tran, H. T., and Simmons, C. P. (2010). A randomized controlled trial of chloroquine for the treatment of dengue in Vietnamese adults. PLoS Negl. Trop. Dis. *4*, e785.

Vankadari, N., and Wilce, J. A. (2020). Emerging WuHan (COVID-19) coronavirus: glycan shield and structure prediction of spike glycoprotein and its interaction with human CD26. Emerg. Microbes Infect. *9*, 601–604.

Walls, A. C., Xiong, X., Park, Y. J., Tortorici, M. A., Snijder, J., Quispe, J., Cameroni, E., Gopal, R., Dai, M., Lanzavecchia, A., et al. (2019). Unexpected receptor functional mimicry elucidates activation of coronavirus fusion. Cell *176*, 1026–1039.

Walls, A. C., Park, Y. J., Tortorici, M. A., Wall, A., McGuire, A. T., and Veesler, D. (2020). Structure, function, and antigenicity of the SARS-CoV-2 spike glycoprotein. Cell *181*, 281–292.

Wan, Y., Shang, J., Sun, S., Tai, W., Chen, J., Geng, Q., He, L., Chen, Y., Wu, J., Shi, Z., et al. (2020). Molecular mechanism for antibody-dependent enhancement of coronavirus entry. J. Virol. *94*, e02015-19.

Wang, H., Yang, P., Liu, K., Guo, F., Zhang, Y., Zhang, G., and Jiang, C. (2008). SARS coronavirus entry into host cells through a novel clathrin- and caveolae-independent endocytic pathway. Cell Res. *18*, 290–301.

Wang, M., Cao, R., Zhang, L., Yang, X., Liu, J., Xu, M., Shi, Z., Hu, Z., Zhong, W., and Xiao, G. (2020). Remdesivir and chloroquine effectively inhibit the recently emerged novel coronavirus (2019-nCoV) in

vitro. Cell Res. *30*, 269–271.
Watanabe, R., Sawicki, S. G., and Taguchi, F. (2007). Heparan sulfate is a binding molecule but not a receptor for CEACAM1-independent infection of murine coronavirus. Virology *366*, 16–22.
Waterhouse, A., Bertoni, M., Bienert, S., Studer, G., Tauriello, G., Gumienny, R., Heer, F. T., de Beer, T. A. P., Rempfer, C., Bordoli, L., et al. (2018). SWISS-MODEL: homology modelling of protein structures and complexes. Nucleic Acids Res. 46, W296–W303.
Xia, S., Liu, M., Wang, C., Xu, W., Lan, Q., Feng, S., Qi, F., Bao, L., Du, L., Liu, S., et al. (2020). Inhibition of SARS-CoV-2 (previously 2019-nCoV) infection by a highly potent pan-coronavirus fusion inhibitor targeting its spike protein that harbors a high capacity to mediate membrane fusion. Cell Res. *30*, 343–355.
Xu, K., Chen, Y., Yuan, J., Yi, P., Ding, C., Wu, W., Li, Y., Ni, Q., Zou, R., Li, X., et al. (2020). Factors associated with prolonged viral RNA shedding in patients with COVID-19. Clin. Infect. Dis. DOI: 10.1093/cid/ciaa351.
Yamamoto, M., Matsuyama, S., Li, X., Takeda, M., Kawaguchi, Y., Inoue, J.I., and Matsuda, Z. (2016). Identification of nafamostat as a potent inhibitor of middle east respiratory syndrome coronavirus S protein-mediated membrane fusion using the split-protein-based cell-cell fusion assay. Antimicrob. Agents Chemother. *60*, 6532–6539.
Yan, R., Zhang, Y., Li, Y., Xia, L., Guo, Y., and Zhou, Q. (2020). Structural basis for the recognition of SARS-CoV-2 by full-length human ACE2. Science *367*, 1444–1448.
Yao, X., Ye, F., Zhang, M., Cui, C., Huang, B., Niu, P., Liu, X., Zhao, L., Dong, E., Song, C., et al. (2020). In vitro antiviral activity and projection of optimized dosing design of hydroxychloroquine for the treatment of severe acute respiratory syndrome coronavirus 2 (SARS-CoV-2). Clin. Infect. Dis. DOI: 10.1093/cid/ciaa237.
Yin, S., Huang, M., Li, D., and Tang, N. (2020). Difference of coagulation features between severe pneumonia induced by SARS-CoV2 and non-SARS-CoV2. J. Thromb. Thrombolysis DOI: 10.1007/s11239-020-02105-8.
Yu, J., Tostanoski, L. H., Peter, L., Mercado, N. B., McMahan, K., Mahrokhian, S. H., Nkolola, J. P., Liu, J., Li, Z., Chandrashekar, A., et al. (2020). DNA vaccine protection against SARS-CoV-2 in rhesus macaques. Science DOI: 10.1126/science.abc6284.
Yuan, S., Jiang, S. C., and Li, Z. L. (2020a). Analysis on possible intermediate hosts of the new coronavirus SARS-CoV-2. Front. Vet. Sci. *7*, 379.
Yuan, S., Jiang, S. C., and Li, Z. L. (2020b). Early oxygen inhalation to prevent SARS-CoV-2-induced acute respiratory distress syndrome. Preprints DOI: 10.20944/preprints202004.0360.v1.
Zhang, B., Zhou, X., Zhu, C., Feng, F., Qiu, Y., Feng, J., Jia, Q., Song, Q., Zhu, B., and Wang, J. (2020). Immune phenotyping based on neutrophil-to-lymphocyte ratio and IgG predicts disease severity and outcome for patients with COVID-19. medRxiv DOI: 10.1101/2020.03.12.20035048.
Zhao, J., Yuan, Q., Wang, H., Liu, W., Liao, X., Su, Y., Wang, X., Yuan, J., Li, T., Li, J., et al. (2020). Antibody responses to SARS-CoV-2 in patients of novel coronavirus disease 2019. Clin. Infect. Dis. DOI: 10.1093/cid/ciaa344.
Zheng, M., and Song, L. (2020). Novel antibody epitopes dominate the antigenicity of spike glycoprotein in SARS-CoV-2 compared to SARS-CoV. Cell. Mol. Immunol. *17*, 536–538.
Zhu, F. C., Li, Y. H., Guan, X. H., Hou, L. H., Wang, W. J., Li, J. X., Wu, S. P., Wang, B. S., Wang, Z., Wang, L., et al. (2020). Safety, tolerability, and immunogenicity of a recombinant adenovirus type-5 vectored COVID-19 vaccine: a dose-escalation, open-label, non-randomised, first-in-human trial. Lancet DOI: 10.1016/S0140-6736(20)31208-3.
Zumla, A., Hui, D. S., Azhar, E. I., Memish, Z. A., and Maeurer, M. (2020). Reducing mortality from 2019-nCoV: host-directed therapies should be an option. Lancet *395*, e35–e36.

Preprints (www.preprints.org) | NOT PEER-REVIEWED | Posted: 21 June 2020 doi:10.20944/preprints202006.0249.v1

LEAD CONTACT AND MATERIALS AVAILABILITY

Requests for material can be directed to Shu Yuan (roundtree318@hotmail.com). All materials and reagents will be made available upon installment of a material transfer agreement (MTA).

METHOD DETAILS

Homology modeling of ACE2 and viral spike proteins

All full-length protein sequences were downloaded from National Center of Biotechnology Information (NCBI; https://www.ncbi.nlm.nih.gov/). The sequence of human angiotensin-converting enzyme 2 (ACE2, Accession ID: BAB40370.1), SARS-CoV CUHK-W1 Spike (S) protein (AAP13567.1) and SARS-CoV-2 WHU01 S protein (QHO62107.1) were subjected to the analysis of homology models which were constructed in the SWISS-MODEL Workspace (Bertoni et al., 2017; Biasini et al. 2014; Bienert et al. 2017; Waterhouse et al. 2018; http://swissmodel.expasy.org/workspace/). The optimal templates for ACE2 was 6m17.1.B with a sequence identity of 99.87% and a coverage from 21-768 aa (805 aa totally). The optimal templates for SARS-CoV S was 6acd.1.A with a sequence identity of 99.83% and a coverage from 18-1119 aa (1255 aa totally). The optimal templates for SARS-CoV-2 S was 6vsb.1.A with a sequence identity of 99.26% and a coverage from 27-1146 aa (1273 aa totally).

The Molecular surface and the electrostatic potential were computed with the Swiss-PdbViewer v4.1.0 software (Bertoni et al., 2017; Biasini et al. 2014; Bienert et al. 2017; Waterhouse et al. 2018). To see every amino acid no matter covered or uncovered by the protein surface, transparency of the surface was set at 30%.

Analysis of antibody epitopes and glycosylation sequons

SARS-CoV CUHK-W1 Spike (S) protein (AAP13567.1) and SARS-CoV-2 WHU01 S protein (QHO62107.1) were subjected to the analysis of antibody epitopes. The sequence-based antibody epitopes score was predicted according to the epitope surface accessibility (SA) by using Emini surface accessibility scale method (Emini et al., 1985; http://tools.iedb.org/bcell/). The possible antibody epitopes were filtered by the surface accessible scores using the default threshold value of 1.0 with a center position of 3 aa and a window size of 6 aa. Then the epitope candidates were re-scored by using BepiPred-2.0 bioinformatic tool with the default threshold value of 0.50 (Jespersen et al., 2017; http://tools.iedb.org/bcell/). The average score of each epitope was calculated based on the epitope score of each amino acid. Epitopes with average scores below 0.5 were ruled out. 27 epitopes were found on SARS-CoV S protein, among which 10 epitopes had been ruled out due to the low epitope scores. 30 epitopes were found on SARS-CoV-2 S protein, among which 9 epitopes had been ruled out due to the low epitope scores. Finally, 17 predicted epitopes for the SARS-CoV S protein and 21 predicted epitopes for the SARS-CoV-2 S protein were screened out and are shown in Tables S1 and S2.

N-linked glycosylation sites in SARS-CoV S and SARS-CoV-2 S are marked on the protein surface based on the sequons identified by Walls et al. (2020).

Prediction of transmembrane domain

Human transmembrane serine protease 2 (TMPRSS2) precursor zymogen (AF123453.1) and cleaved active enzyme (AAK29280.1), human ACE2 (BAB40370.1), SARS-CoV CUHK-W1 S protein (AAP13567.1) and SARS-CoV-2 WHU01 S protein (QHO62107.1) were subject to the transmembrane domain analysis. The putative transmembrane helices were scored by using TMHMM Server v. 2.0 bioinformatic tool (Krogh et

 doi:10.20944/preprints202006.0249.v1

al., 2001; Moller et al., 2001; http://www.cbs.dtu.dk/services/TMHMM/).

Alignment of SARS-CoV and SARS-CoV-2 spike proteins

In a phylogenetic network analysis of SARS-CoV-2 genomes, three central variants distinguished by amino acid changes were defined, which we have named A, B, and C types (Forster et al., 2020). Three representative S protein sequences of SARS-CoV-2 USA-WA1/2020 (QHO60594.1) for the type A virus strain, SARS-CoV-2 WHU01 (QHO62107.1) for the type B virus strain and SARS-CoV-2 SNU01 (QHZ00379.1) for the type C virus strain were collected. Along with the SARS-CoV CUHK-W1 S protein sequence (AAP13567.1), these four amino acid sequences were aligned using the software ClustalX2.1 (Larkin et al., 2007).

QUANTIFICATION AND STATISTICAL ANALYSIS

Clinical data of cancer patients with confirmed SARS-CoV-2 infections (Montopoli et al., 2020) were re-analyzed. One-way analysis of variance (ANOVA) was used to test for statistical significance. Only p values of 0.05 or lower were considered statistically significant. For all statistical analyses, the SPSS 22.0 software package was used.

DATA AND CODE AVAILABILITY

The study did not generate unique datasets or code.